On Depolarization of Visible Light from Water Clouds for a Monostatic Lidar

KUO-NAN LIOU

Institute for Space Studies, Goddard Space Flight Center, NASA, New York, N. Y. 10025

11 November 1971 and 23 February 1972

Lidar (laser radar) has recently been employed in probing terrestrial clouds and aerosols to obtain useful information on their composition and structure (see, e.g., Herman *et al.*, 1971; Liou and Schotland, 1971). Liou and Schotland (hereafter referred to as LS) have proposed that the returned depolarization from a monostatic lidar can be used as a quantity for distinguishing between water and ice clouds. Measurements made by Schotland *et al.* (1971) have demonstrated the usefulness of this depolarization technique.

In LS, use was made of the theoretical Gamma functions suggested previously by Deirmendjian (1964) for cloud drop-size distributions to perform the scattering computations. However, the observed cloud drop-size distributions are often remarkedly different from Deirmendjian's models, especially in the tail regions of the large particles. After an extensive survey of the published literatures on the measurements of cloud drop-size distributions, typical droplet spectra of six major cloud types were chosen for the light-scattering calculations. It is the purpose of this note to investigate if there are any differences in the values of backscattering and depolarization by utilizing the theoretical cloud models and the observed drop-size distributions.

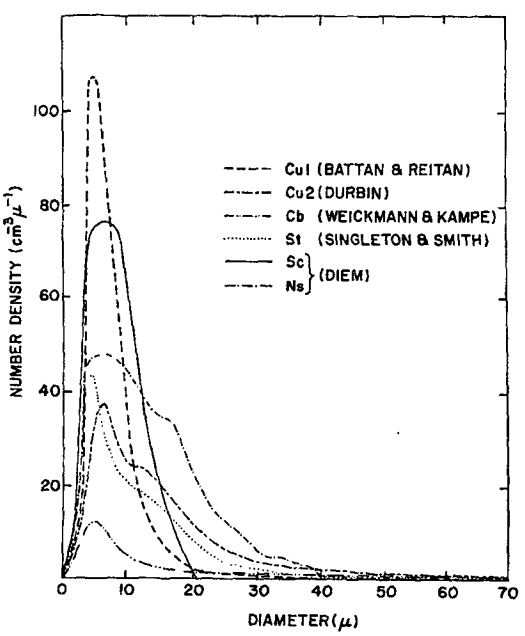

FIG. 1. The observed drop-size distributions for six major cloud types. The curves are presented in such a way that the integral of the area under each curve equals the total particle number density.

The drop-size distribution for fair weather cumulus (Cu 1) is based on the observations by Battan and Reitan (1957), while that for cumulus congestus (Cu 2) is taken from measurements made by Durbin (1959) for cumulus clouds. The drop-size distribution for cumulonimbus (Cb) is that reported by Weickmann and aufm Kampe (1953), while that for stratus (St) is chosen from measurements made by Singleton and Smith (1960) for layer clouds. Finally, the drop-size distributions for stratocumulus (Sc) and nimbostratus (Ns) are based on a series of observations obtained by Diem (1948). The above six size distributions are shown in Fig. 1, the curves being presented in such a way that the integral of the area under each curve is equal to the total particle concentration indicated in Table 1. Cloud groups C4 and C8 are explained later. It is seen that the size distributions for Cu 1 and Sc are rather narrow and drop off rapidly, while those for Cu 2, Cb, St and Ns are very broad with the number of particles in the tail regions being significant.

Mie scattering computations for polydisperse water drops were carried out by using the drop-size distributions shown in Fig. 1. Gaussian integration for the particle size was employed in which the integrations over the drop radii were performed to an upper limit listed in the fourth column of Table 1. The integration increments were chosen small enough to make the phase function smooth (Dave, 1969).

Fig. 2 illustrates the phase functions for the six cloud types discussed previously. The phase functions

TABLE 1. Droplet parameters for six cloud types, and cloud groups C4 and C8.

Cloud type	Author	Concentration (cm^{-3})	Drop radius (μ)	Water content ($gm\ cm^{-3}$)	Scattering cross section $\bar{\sigma}_s$ ($10^{-8}\ m^2$)
Cu 1	Battan and Reitan	293	0–20	0.33	0.01659
Cu 2	Durbin	207	0–40	0.66	0.04683
Cb	Weickmann and Kampe	75	0–70	2.50	0.04816
Sc	Diem	350	0–12	0.09	0.01204
Ns	Diem	330	0–20	0.40	0.04101
St	Singleton and Smith	178	0–40	0.78	0.04731
C4	Deirmendijan	—	0–17	—	0.01682
C8	Deirmendjian	—	0–17	—	0.06007

are normalized such that

$$\frac{1}{4\pi}\int_{4\pi} P_{1,2}(\theta)d\Omega=1, \tag{1}$$

where θ is the scattering angle, Ω the solid angle, and P_1 and P_2 the components of phase function perpendicular and parallel, respectively, to the scattering plane. We have used an incident wavelength of 0.6943 μ (red light) throughout the computations. Since the mean size parameters (the ratio of the circumference of a drop to the incident wavelength) are quite large ($\gtrsim 50$) for all six size distributions, we could explain the features that occurred in the phase functions by means of ray optics (Liou and Hansen, 1971). The peaks in the phase functions at the scattering angle $\theta \approx 0°$ are the results of Fraunhofer diffraction which is formed by rays passing by the drops. The strong maxima at $\theta \approx 140°$ are the primary cloudbows which arise from rays internally reflected once in the drops. In addition, the second cloudbow at the scattering angle of $\sim 125°$ is due to rays undergoing two internal

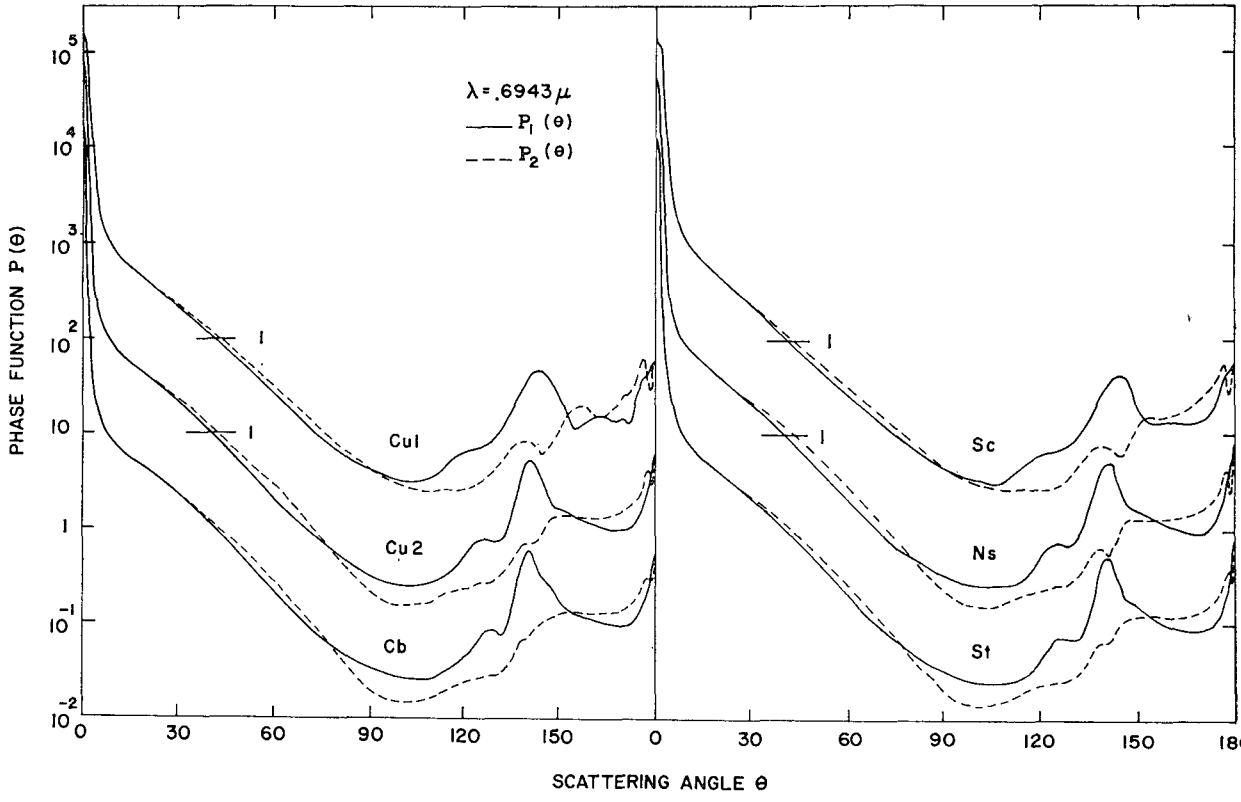

FIG. 2. Single-scattering phase functions perpendicular (solid lines) and parallel (dotted lines) to the scattering plane for the observed drop-size distributions illuminated by 0.6943 μ radiation. The vertical scales apply to the lowermost curves (Cb and St), while the scales for the other curves can be obtained by dividing by a factor of 10 such that the horizontal bar on each curve occurs at unity.

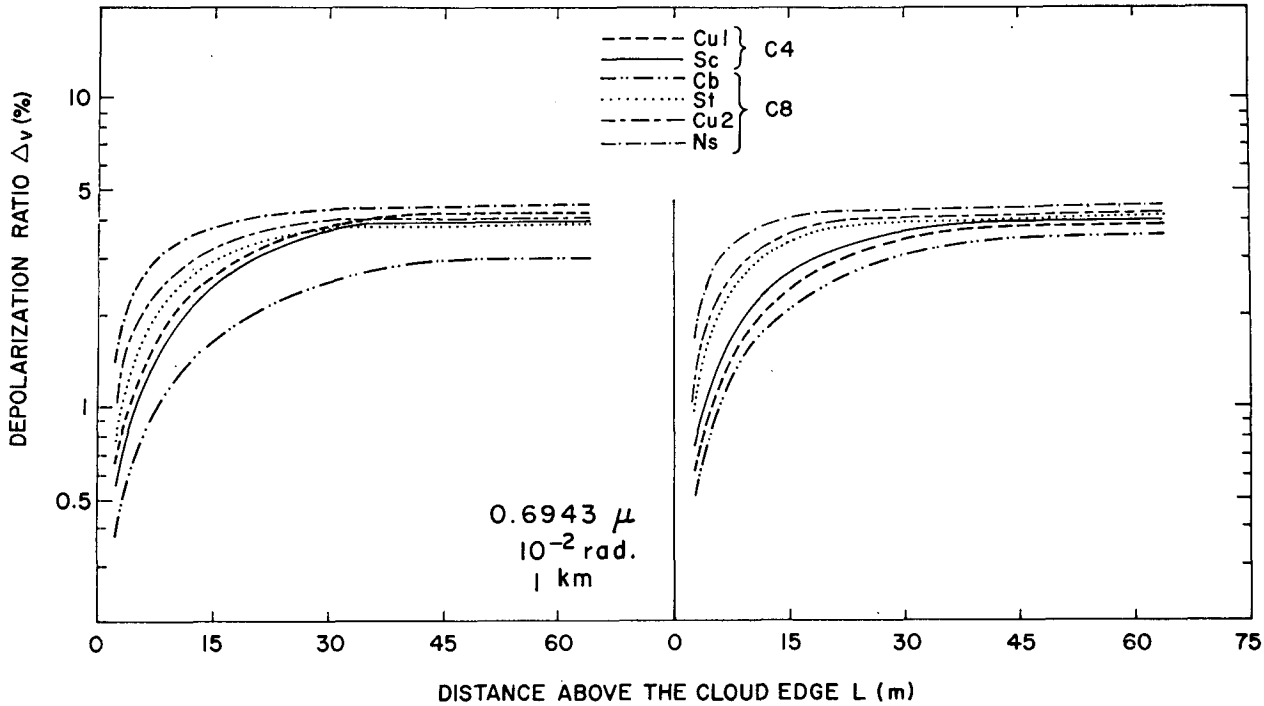

FIG. 3. The depolarization ratio as a function of distance above the cloud edge. The left-hand side illustrates the results obtained by using observed drop-size distributions, while the right-hand side shows the results obtained by using theoretical cloud models C4 (replacing Cu 1 and Sc) and C8 (replacing Cb, St, Cu 2 and Ns) with the same particle number densities given in Table 1.

reflections in the drops. This feature is more pronounced in Cu 2, Cb, St and Ns than in Cu 1 and Sc because the mean size parameters of the former are larger than those of the latter. Moreover, the glory at $\theta \approx 180°$ is caused by the backscattering from edge rays which possibly are associated with surface waves generated on the drops.

The computed mean scattering cross sections for the six cloud types are presented in the last column of Table 1. In view of the values of phase functions and mean scattering cross sections (which are independent of the particle concentrations), we divide the six cloud types into two groups. The first consists of Cu 1 and Sc which have scattering properties similar to those of Deirmendjian's (1964) cloud model at mode radius of 4 μ (C4), while the second includes Cu 2, Cb, St and Ns which have scattering properties approximately similar to those of C8. The phase functions for cloud models C4 and C8 were given in LS and will not be reproduced here.

Now we would like to see if there are any distinctions in the depolarization ratios of the scattered visible light from clouds for a monostatic lidar by employing the observed drop-size distributions instead of the theoretical cloud models. In the computations discussed below, we use the first and the second groups to replace the cloud models C4 and C8, respectively, with the same particle concentration (see Table 1) in both cases.

The depolarization ratio of a vertically polarized outgoing beam for all orders of backscattering can be expressed as

$$\Delta_v = \sum_{n=2}^{\infty} P_y^{(n)} \Big/ \sum_{n=1}^{\infty} P_x^{(n)}, \qquad (2)$$

where the superscript n denotes the order of backscattering, e.g., $n=1$ represents the primary backscattering, P_x is the received power which retains the polarization of the incident energy, while P_y is that of the cross-polarized component. A similar definition can be obtained for a horizontally polarized outgoing beam. The computations for the secondary ($n=2$) backscattering have been illustrated in detail by LS, while for those order of scattering higher than the second, we adopt the method described by Liou (1971).

For the purpose of illustration, we employ a receiver beam width of 10^{-2} rad and a distance between the cloud edge and the receiver of 1 km in the following calculations. The left- and right-hand sides of Fig. 3 show the results of the depolarization ratio computations using the six observed drop-size distributions and the theoretical cloud models, respectively. The differences between the values of the two kinds of computations are found to be rather small ($<0.5\%$); consequently, the effects of the size distribution can be declared as insignificant.

Based upon the above results, we therefore conclude that for all practical purposes in backscattering and

depolarization calculations, we may use cloud model C4 to represent clouds such as fair weather cumulus, and cloud model C8 to represent clouds such as cumulus congestus, cumulonimbus, etc. Hence, in this short note, we have demonstrated that the theoretical analyses and conclusions presented by LS can be applied reasonably well to naturally occurring terrestrial water clouds.

Finally, we would like to point out that although the depolarization technique described by LS can be used to distinguish between the ice and liquid phase of cloud particles, the use of this technique to obtain information regarding the size distribution and the number density of cloud elements would appear to be difficult. Therefore, other methods should be designed to accomplish the sensing of cloud composition regarding the above two aspects of the problem.

Acknowledgments. I am grateful to Prof. R. M. Schotland for reviewing this note and for making several useful criticisms. During the course of this research, I held a NRC-NAS Research Associateship supported by NASA.

REFERENCES

Battan, L. J., and C. H. Reitan, 1957: Droplet size measurement in convective clouds. *Artificial Stimulation of Rain*, London, Pergamon Press, 184 pp.

Dave, J. V., 1969: Effect of coarseness of the integration increment on the calculation of the radiation scattered by polydispersed aerosols. *Appl. Opt.*, **8**, 1161–1167.

Deirmendjian, D., 1964: Scattering and polarization properties of water clouds and hazes in the visible and infrared. *Appl. Opt.*, **3**, 187–196.

Diem, M., 1948: Messungen der Frosse von Wolkenelementen II. *Meteor. Rundschau*, **9**, 261–273.

Durbin, W. G., 1959: Droplet sampling in cumulus clouds. *Tellus*, **11**, 202–212.

Herman, B. M., S. R. Browning and J. A. Reagan, 1971: Determination of aerosol size distribution from lidar measurement. *J. Atmos. Sci.*, **28**, 763–771.

Liou, K. N., 1971: Time-dependent multiple backscattering. *J. Atmos. Sci.*, **28**, 824–827.

——, and J. E. Hansen, 1971: Intensity and polarization for single scattering by polydisperse spheres: A comparison of ray optics and Mie theory. *J. Atmos. Sci.*, **28**, 995–1004.

——, and R. M. Schotland, 1971: Multiple backscattering and depolarization from water clouds for a pulsed lidar system. *J. Atmos. Sci.*, **28**, 772–784.

Schotland, R. M., K. Sassen and R. Stone, 1971: Observations by lidar of linear depolarization ratios for hydrometeors. *J. Appl. Meteor.*, **10**, 1011–1017.

Singleton, F., and D. F. Smith, 1960: Some observations of drop size distributions in low layer clouds. *Quart. J. Roy. Meteor. Soc.*, **86**, 454–467.

Weickmann, H. K., and H. J. aufm Kampe, 1953: Physical properties of cumulus clouds. *J. Meteor.*, **10**, 204–211.